





## TUTORIAL REVIEW

View Article Online  
View Journal | View Issue



Cite this: *Environ. Sci.: Processes  
Impacts*, 2025, 27, 878

# A global review of long-range transported lead concentration and isotopic ratio records in snow and ice†

Hanna L. Brooks, <sup>‡\*ab</sup> Kimberley R. Miner, <sup>bc</sup> Karl J. Kreutz <sup>ab</sup>  
and Dominic A. Winski <sup>ab</sup>

Lead (Pb) has been used for centuries in currency, transportation, building materials, cookware, makeup, and medicine. Mining of Pb in the Roman era matched the ever-increasing demand for metallurgy, transportation, and industry, resulting in a marked deposition of human activity in the geologic record. Researchers use global snowpacks and ice cores to study the historic anthropogenic use of Pb and subsequent deposition into the environment. As the cryosphere resources erode with climate warming, there is an increased urgency to map the content and source of Pb distribution in the environment. In this systematic literature review, we examine studies of long-traveled background atmospheric lead signals in natural, undisturbed snowpacks and ice cores globally. After a systematic review of the literature, we have synthesized 165 published papers to contextualize current data availability and examine spatial and temporal coverage of existing long-range transported Pb records. Cumulatively, these papers contain 560 records for individual and transect sample sites. Of these site records, 147 are ice core analyses, 389 are from snowpits, and 24 span the snow to ice transition. The records are globally distributed, with a high concentration of records at the poles and fewer records at low latitude alpine sites. Long timescale records are available from the Greenland and Antarctic ice sheets (>100 000 years). Shorter timescale records are available for alpine glaciers (>15 000 years) and persistent snowpacks (generally <5 years). To illustrate the research potential of these records, we selected key global records to analyze and contextualize the Pb pollution record from the North Pacific, noting its unique record of China's industrial revolution and the subsequent explosion of industrial output from China over the last 45 years. Finally, we provide recommendations for future studies aimed at reducing current temporal and spatial gaps in the records. We suggest analyzing archived ice cores never before analyzed for Pb, focused proposals on regions with critical data gaps, continuous resampling of sites to include modern Pb emission sources, and use of analysis techniques which have low sample preparation requirements, high sensitivity, and capability for ultra-trace concentration Pb analysis.

Received 4th September 2024  
Accepted 20th September 2024

DOI: 10.1039/d4em00526k

rsc.li/espi

## Environmental significance

For centuries, anthropogenic activity has been responsible for inputting Pb, and other trace metals, into the environment. As a highly toxic metal with known negative effects on human health, it is critical to understand the amount of Pb being released into the environment, sources of Pb emissions, and how these factors have evolved over time. In this study, we compile published records of long-range transported Pb analyzed from the cryosphere (ice and snow). With this collated set of records, researchers will now be able to quickly evaluate which records will be pertinent to their research questions. Questions regarding regional, inter-regional, and global comparisons of the amount of Pb deposited in the environment and the major Pb sources through time can be examined without a lengthy review of the literature. Additionally, examining these records as a whole highlights spatial and temporal data gaps which are currently limiting our understanding of changes to anthropogenic Pb emissions. As climate change remobilizes legacy Pb into water sources and oceans, understanding the amount of legacy Pb trapped in the cryosphere is necessary to mitigate impact on human health.

<sup>a</sup>School of Earth and Climate Sciences, University of Maine, Orono, Maine, USA.  
E-mail: hanna.brooks@maine.edu

<sup>b</sup>Climate Change Institute, University of Maine, Orono, Maine, USA

<sup>c</sup>Jet Propulsion Laboratory, California Institute of Technology, California, USA

† Electronic supplementary information (ESI) available. See DOI: <https://doi.org/10.1039/d4em00526k>

‡ Present address: Department of Geology, Amherst College, Amherst, Massachusetts, USA.

## 1 Introduction

Lead (Pb) is a naturally occurring heavy metal,<sup>1</sup> found as a trace element in the Earth's upper crust ( $17 \times 10^{-6} \text{ g g}^{-1}$ ).<sup>2</sup> The primary natural sources of Pb in the crust are hydrothermal veins, volcanogenic sedimentary deposits, and hydrothermal



and marine deposits.<sup>1</sup> Critically, Pb isotope ratios (*e.g.*,  $^{206}\text{Pb}/^{207}\text{Pb}$ ,  $^{208}\text{Pb}/^{206}\text{Pb}$ ) are fixed through physiochemical processes, including ore extraction, smelting, and combustion of fossil fuels, and are not modified during atmospheric transportation or deposition.<sup>3</sup> Therefore, Pb isotope ratios in paleoclimate records provide a long-term record of changes to emission sources through time.<sup>4–7</sup>

Cryosphere (ice core and snowpack) paleoclimate records encompass hundreds to thousands of years of depositional time; identifying the historic natural and anthropogenic variation of Pb.<sup>4,8</sup> Any use changes by human culture that changes the gross Pb concentration or alters the pollution source(s) can be examined using these paleorecords.<sup>4,5,9,10</sup> For example, high-altitude European ice cores and snowpack sites record the onset of Greco-Roman mining and smelting activity<sup>11</sup> and the Industrial Revolution.<sup>4</sup> The sudden population decrease resulting from the Black Plague caused a swift cessation of mining and smelting across Europe. This event was recorded in the Colle Gnifetti glacier in the Swiss Alps, as a dramatic decrease in Pb concentration.<sup>12</sup> In more recent times, the impact of adding tetraethyl lead to gasoline, and its subsequent global phase-out can be observed globally.<sup>7,10,13</sup>

However, these cryosphere paleorecords are threatened by climate change.<sup>14</sup> Higher temperatures accelerate the melting of ice, snow, and permafrost in the cryosphere.<sup>14–16</sup> Many of the cryosphere sites most vulnerable to increased effects of climate change reside in areas where Pb data is already scarce, primarily low-latitude sites and mountain glaciers.<sup>14</sup> Additionally, the increase in meltwater from these sites poses increased health risks. As meltwater moves through the environment, it carries remobilized historic trace metals, including Pb.<sup>17,18</sup> This legacy Pb is subsequently remobilized in the downstream environment, eventually ending in critical human water sources and oceans.<sup>15–17,19</sup>

This tutorial review aims to synthesize globally distributed records of long-range transported Pb concentration and isotope ratios in the cryosphere, evaluate regional coverage, provide context for differences in regional trends (*e.g.*, North Atlantic *vs.* North Pacific), and identify critical research needs. This systematic literature review is the most extensive global examination of published records (including 559 sample areas, published in 165 papers) of Pb ice core and snowpack data compiled to date. Here, we have synthesized 165 published papers to contextualize current data availability and examine spatial and temporal coverage of existing long-range transported Pb records. Our hope is that, using the compiled records, researchers will be able to quickly filter available records<sup>20</sup> to match selection criteria, mitigating lengthy literature searches, and enabling local, regional, and international Pb emissions and transportation comparisons.

## 2 Why do we care about Pb?

### 2.1 History of human use

Pb is found globally in raw materials (*i.e.*, raw ore and fossil fuels) and industrial/commercial products.<sup>9,21</sup> Through time, anthropogenic use of these materials in evolving ways has left

a direct imprint on the environment. The earliest known spikes in Pb traced in paleoclimate records have been tied to mining and metallurgy. Pb was developed as a smelting agent at different times regionally: ~6500–6400 BCE (Great Lakes Region, North America, and Turkey), 2800 BCE (Liangzhai Lake, central China), 1000 BCE (Iberian Peninsula), and 400 CE (pre-Incan Bolivia).<sup>9,22</sup> During the Early Bronze Age (~3000 BCE), most Pb was produced as a by-product of silver refining during cupellation. Cupellation is a refining process by which precious metals (*i.e.*, gold, silver) are separated from base metals (*i.e.*, lead, copper) using very high heat.<sup>9</sup> Use of Pb in commercial products continued to rise during the Roman Empire, as Pb was used in currency, weights, pipes, glassmaking, ceramics glazes, cooking pots, makeup, and medicine.<sup>9</sup> Pb emissions rose dramatically as nations industrialized, beginning with the United States and Western Europe in mid-17th century to the early 19th century.<sup>23</sup> By the 20th century, roughly half of the lead produced was used in vehicles, as a critical component in car batteries, and in gasoline as tetraethyl lead ( $(\text{CH}_3\text{CH}_2)_4\text{Pb}$ ). In 2021, leaded gasoline for cars and trucks was phased out worldwide, but leaded fuels are still used in small aircraft aviation, motorsports and off-road vehicles.<sup>24</sup> All fuel continues releasing small concentrations of Pb into the atmosphere, even when labeled as ‘unleaded’.<sup>21</sup>

While the high-temperature industrial processes that emit Pb emissions are well known (*e.g.*, metal smelting, refuse incineration), the worldwide use of these processes is not well-tracked.<sup>21,22</sup> In industrialized nations, yearly emissions estimates (Fig. 1) are compiled by source and pollutant for the United States,<sup>25–28</sup> the European Union,<sup>29</sup> Canada,<sup>30</sup> and China.<sup>31,32</sup> Reported yearly Pb emissions estimates indicate a steady decrease across Europe, North America, and Russia

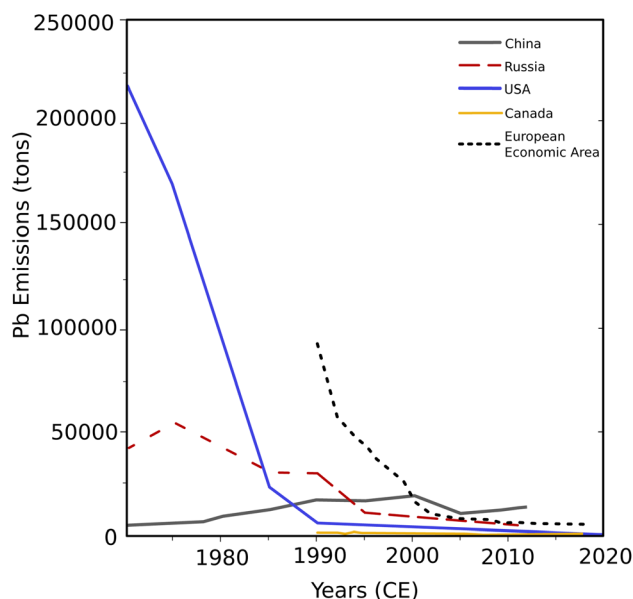


Fig. 1 Pb emissions in metric tons for several major industrialized nations from 1970 to 2020.<sup>22,25–31</sup> For many countries, data only existed once the harmful nature of leaded gasoline was recognized and phased out in the 1990s.



since the 1970s (Fig. 1). This decrease has been driven by legislation that prohibited tetraethyl leaded gasoline, improvements in the efficiency of coal combustion, and advances in non-ferrous metal smelting technology.<sup>4,9,21,33</sup> Critically, over the same period, Pb emissions from China largely increased.<sup>31</sup> In newly dev in newly developed countries, rising Pb emissions stem from increasing resource demand and human population growth in the mid-20th century.<sup>4,21</sup>

Some limited data (such as leaded gas usage) is available for countries such as Australia<sup>34</sup> and Brazil.<sup>35</sup> Direct assessments of the global Pb aerosol emissions into the atmosphere are logistically complicated, time-consuming, and must be updated as Pb use changes over time (*e.g.*, phase-out of leaded gasoline, technological advancement).<sup>36–38</sup> Therefore, to constrain the use, emission, and impacts of Pb in the environment, emission estimates rely on models and environmental data records (*i.e.*, ice, snow, soils, lakes) when direct, observational atmospheric data is unavailable.<sup>21</sup>

## 2.2 High Pb concentrations directly impacts health

Pb's adverse health and environmental effects were already known during Roman times: smelting furnaces were placed on the top of hills, as placing them where the fumes would blow across the land led to "spoiled vegetation and poisoned soil".<sup>9</sup> Formal medical descriptions for lead poisoning or lead colic are recorded as early as 370 BC.<sup>4,22</sup> Modern medicine understands that Pb exposure at all levels has toxic effects on many organ systems.<sup>4,22</sup> Critically, 10% of the Pb that passes through adults is absorbed, compared to 50% in children, leading to increased severity from exposure.<sup>39</sup> Uptake routes include inhalation and oral ingestion, allowing Pb to be stored in bone marrow.<sup>40</sup>

The U.S. Environmental Protection Agency has established a maximum daily consumption of Pb to 10 µg daily.<sup>40</sup> However, due to the risk to reproductive health, some U.S. states set a maximum limit of 0.5 µg daily.<sup>40</sup> Pb poisoning targets the nervous, cardiovascular, gastrointestinal, genitourinary, and hemopoietic systems.<sup>39,40</sup> Pb readily crosses the blood–brain barrier into the brain tissue (depositing in the cortex and hippocampus) and can also deposit into bones. Pb deposition can also be transferred from mother to child within the placenta.<sup>39</sup> Even at low levels, Pb can cause nausea, fatigue, headache, irritability, tremors, memory loss, and joint and muscle pains.<sup>22,39</sup> At high exposures, Pb can cause permanent behavioral and neurological problems, developmental delays in children, motor deficits, slowed bone growth, spontaneous abortions in the first trimester, encephalopathy, and death.<sup>9,21,22,39,40</sup> Despite known health effects, Pb remains common in cosmetics (*i.e.*, lipstick, hair dye), building materials (*i.e.*, roofing, old plumbing, old paint), welding/solder, in automobiles (*i.e.*, car batteries), bullets, children's play products (*i.e.*, crayons, playing dough).<sup>22,41</sup>

## 2.3 Global dispersal and entrainment

Pb is released and evaporates into the atmosphere through natural (*i.e.*, volcanoes, dust) and anthropogenic sources (*i.e.*, production of industrial/consumer goods, combustion of fossil

fuels, refuse incineration, chemical spills, and leaching in landfills).<sup>21</sup> Aerosolization allows Pb particles to be transported long distances (>100 km) with sea salt spray, aeolian dust, or condensation of atmospheric gas in the troposphere.<sup>42,43</sup> Aeolian dust is particularly suited to carry sub-micron particles of air pollutants, including Pb, for 5 to 10 days<sup>44,45</sup> (and thousands of kilometers) within the atmosphere in wind currents.<sup>42,43,46,47</sup> The distance atmospheric particles are transported before deposition depends on these aerosols' physical and chemical properties, including particle size, shape, mass, and composition.<sup>4</sup> As snow is transformed into ice, a high temporal resolution record with an annual chronology is recorded.<sup>4,48</sup> Five-day back trajectories (120 hours; Fig. 2) from HYSPLIT<sup>49</sup> show that while a given site records a local regional signal, it also captures the signal from surrounding regions, corresponding to the local climatology and prevailing wind direction. Careful site selection allows researchers to build a local, regional, and inter-regional image of changing pollution sources through time. For example, detailed examinations of Arctic sites record changes in North American, European, and Asian Pb.<sup>6–8,51–55</sup> Studies of sites in Antarctica and South America can record Antarctic, South American, and Australian Pb sources.<sup>56–60</sup> Asian study sites reveal changes in Pb sources from Eastern Europe, Asia, and Africa.<sup>61–63</sup> Layering sites and regions, as in Fig. 2 Panel F, would allow for global examination of Pb. However, the major data gaps in Asia, South America, and Africa (Fig. 3) hinder efforts to assess the impact of Pb deposition on a global scale.<sup>22,66</sup> Pb deposition occurs through either dry (*i.e.*, gravitational settling) or wet deposition (*i.e.*, precipitation) processes in sedimentary environments.<sup>4,67</sup> Sedimentary Pb records in lakes, peat, bogs, and snow/ice fields receive primarily atmospheric input and are geomorphically stable. Ice cores and snowpacks are considered the 'gold standard' for studying historic emission records, since cold conditions and low concentrations of chemical impurities impede signal migration post-deposition in ice.<sup>22,68</sup> Once deposited on the surface and incorporated into various sedimentary environments (*e.g.*, glaciers, peatlands), Pb is chemically immobile, providing a historical record of metal pollution.<sup>66,69</sup> Any disruption to the equilibrium of the substrate within which the lead has settled can cause re-mobilization.<sup>67</sup> Pb and other pollutants' major re-mobilization in the cryosphere occurs as discharge in meltwater discharge.<sup>67,70</sup> Melt effectively reintroduces historic pollution into downstream environments,<sup>15–17,19</sup> impacting the biological productivity and ecology of the system, especially at top trophic levels.<sup>70–72</sup> Reintroduction of historic pollution therefore poses a large risk to human health. As meltwater increases, transported Pb concentrations increase, creating a higher risk of severe Pb poisoning in communities using glacial meltwater and snowmelt drinking sources.<sup>9,22,40,71</sup> Previous studies have identified monitoring of increased air surface temperatures and resultant glacial melt as an ecological priority.<sup>15–17,19,66,71</sup> High-temperature industrial processes emit several metals simultaneously (*e.g.*, ferrous metallurgy which emits Pb, Zn, Ni, Cd, Cr, & Hg).<sup>22</sup> Therefore, Pb records can also be a proxy for other metal emissions, providing an understanding of metal pollution overall.<sup>22</sup>



## Hysplit 120 Hour Backtrajectories from the 2010s

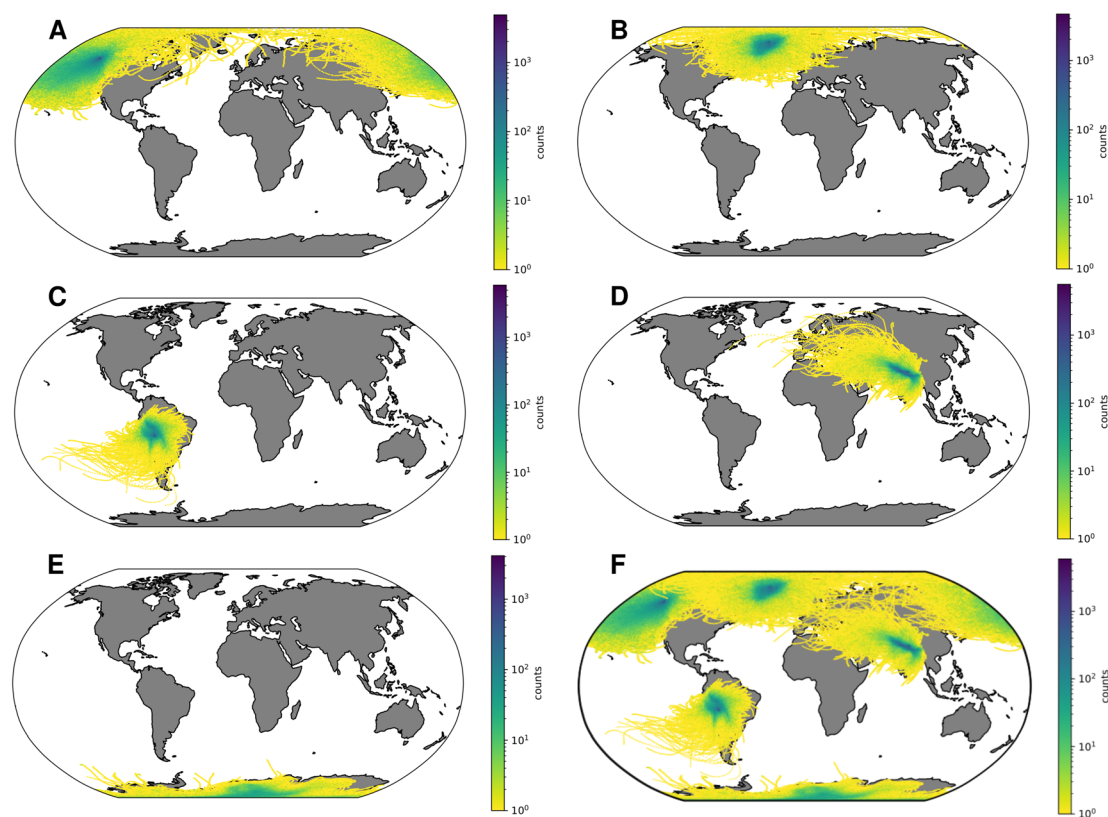


Fig. 2 Calculated 5 day (120 hour) back trajectories showing the wind path to different ice core sites generated using the NOAA HYSPLIT Trajectory Model.<sup>49,50</sup> One trajectory path is plotted per day for the period from 2010 to 2019. This decade was examined as it provides context to the start of the leaded gasoline phase out. The trajectories plotted are generally representative of wind patterns from 1949 to 2022. See ESI Fig. 2† to compare with trajectories from the 1970s. The trajectories have been transformed into a hexbin map, colored to indicate the number of trajectories within a given hex. Panel (A) shows the trajectories for Mt. Logan, Canada (60.59 N, 219.5 W), (B) is Summit, Greenland (72.967 N, 38.067 W), (C) is Illimani, Bolivia (16.617 S, 68.067 W), (D) is Qomolangma (Everest; 28.05 N, 87.6 E), (E) is the South Pole (90 S, 0 E), and panel (F) shows a combination of (A–E).

To correctly interpret the deposited Pb signal, researchers must also consider the temporal context of sites. The more static, long-lasting ice sheets of Greenland and Antarctica contain Pb signals that extend beyond the onset of human pollution: 155 kyr B.P.<sup>73</sup> and 801.5 kyr B.P.,<sup>74</sup> respectively. High alpine ice cores can capture decades, centuries, or even thousands of years of Pb data.<sup>48,68</sup> Whereas yearly data can be collected in locations with permanent or semi-permanent snowpacks and little melt.<sup>75–77</sup> Pb analyses in snow and ice samples are biased towards the poles and high-altitude alpine sites in Europe (Fig. 3), with minimal analyses focused on high-altitude, low-latitude mountain regions, leaving gaps in the temporal and spatial record (see Section 4). As melting accelerates throughout the cryosphere (*i.e.*, Tibetan Plateau<sup>78</sup>), researchers have begun focused efforts to study areas vulnerable to climate change impacts before the records disappear.<sup>14,79</sup> Many of the sites endangered by climate change reside in regions where major regional-scale data gaps exist. Additional focus on sites endangered by climate change is necessary to begin quantifying the increased risk to downstream drinking water sources and associated health risks.<sup>4,22,40,71</sup>

#### 2.4 Determining Pb levels in snow and ice

In the 1950s, improved procedures to reduce anthropogenic contamination during sampling and analysis of ice and snow<sup>9,10,80</sup> provided the first records illustrating natural levels of Pb *vs.* anthropogenic emissions in various reservoirs.<sup>81–84</sup> In the following decades, data was collected and analyzed worldwide, including aerosols in the atmosphere,<sup>36,37</sup> peat cores,<sup>85,86</sup> lakes,<sup>87,88</sup> and snow and ice fields (Table 1, ESI†<sup>20</sup>).

Modern methods (Table 1, ESI†<sup>20</sup>) allow examination of Pb in snow and ice where Pb concentrations are trace values ( $10 \times 10^{-9} \text{ g g}^{-1}$ ). Even at these low composition values, these methods can also accurately analyze isotopic ratios. Inductively coupled plasma mass spectrometry (ICP-MS) instruments are sensitive enough to analyze Pb isotopes in snow and ice<sup>89,90</sup> with multiple sample introduction methods to enhance data quality and reduce sample preparation requirements.<sup>91–99</sup> Promising new developments for ICP-MS methodologies include sub-nanogram detection limits *via* ICP-MS with a jet interface pump,<sup>100</sup> inline octopole reaction cells (ICP-MS/MS) for the removal of isobaric interferences,<sup>4,13,101,102</sup> time of flight mass





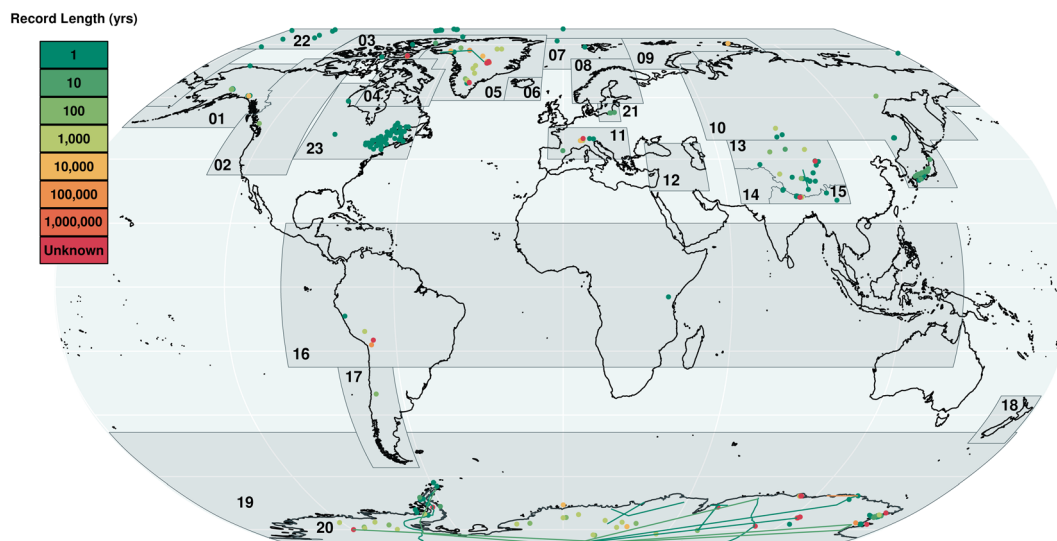


**Fig. 3** The Robinson map projection shows the global records of Pb concentration and isotopes from Tables A.1 and A.2.† Sampling sites for Pb work in snow and ice are colored by temporal length. When samples were collected as a traverse, the path is illustrated as a solid line as the best approximation. Note: some traverse lines have artifacts due to incomplete trip logistical data. For ease of discussion, the Pb records are broken into 23 regions, the 20 first-order regions from the Global Terrestrial Network for Glaciers,<sup>64</sup> plus three author-defined regions. These regions are mapped on the figure with grey boxes, labeled with their numerical glaciated region code (*i.e.*, 01 for Alaska). See Table 1 for a complete list of glacier region names and codes. To see how these sample sites compare to the known glaciers mapped in the Randolph Glacier Inventory,<sup>65</sup> see ESI figure.†<sup>20</sup>

spectrometry (ICP-TOF-MS) on ultra-trace concentration samples.<sup>103</sup> At ultra-low concentrations ( $<5 \times 10^{-12} \text{ g g}^{-1}$ ),<sup>104</sup> laser atomic fluorescence spectrometry,<sup>105,106</sup> thermal ionization mass spectrometry (TIMS),<sup>107,108</sup> isotope dilution thermal ionization mass spectrometry (ID-TIMS),<sup>109</sup> and secondary-ion mass spectrometry (SIMS)<sup>110</sup> analyses are used to calculate exact isotopic ratios. However, these methods are limited by extensive sample preparation requirements. Novel combined scanning electron microscopy and energy-dispersive X-ray spectroscopy (SEM-EDS<sup>111</sup>) may provide researchers a new method for the direct measurement of Pb in snow and ice.

### 3 Reviewing global long-range transported Pb records from the cryosphere

After systematically reviewing the literature, we have assembled and organized all available Pb long-range transported depositional records (as of this writing, June 2024) from snow pits and ice cores (ESI†<sup>20</sup>). These tables provide the record metadata, including sampling site location, analysis method, and temporal scope. All systematic literature review methods are detailed in ESI 1,† including database search parameters, selection criteria and citations of included records. Critically, we have only included records with long-range transported Pb deposition. All records of Pb source signatures (volcanic ash, bedrock, ore, coal, leaded gasoline, aerosols, *etc.*) have been excluded from the curated records. Researchers querying the records need to access suitable potential local contributions and other sources of Pb, and include them in data analysis.<sup>4-7</sup>

These Pb sources will be site specific, as source contributions vary regionally and globally.<sup>4,5</sup> Combining the collated records (ESI†<sup>20</sup>) and Pb source information from select spatial or temporal areas of interest, researchers will be able to quickly examine differences attributed to fluctuating pollution sources and the marked effects of human choices on the environment.<sup>4-7</sup>

This review seeks to collate published 560 site records (from 165 published papers), and to examine spatial and temporal coverage. For clarity, records of individual sample sites were separated from records collecting samples along transects (ESI†<sup>20</sup>). Together, these long-range Pb depositional records account for 413 individual sites and 16 transects, representing thousands of years of Pb data collected globally by hundreds of researchers. We examined the spatial and temporal coverage of the records by splitting the analyses into 23 global regions (see Table 1; Fig. 3). Fig. 3 provides a visual representation of the records and the global regions. Here, the known glaciers included in the Randolph Glacier Inventory<sup>65</sup> are marked with light blue dots, and the Pb records are marked in orange. Quickly, areas where sampling was primarily sea ice (*i.e.*, region 22), ice sheets (*i.e.*, regions 05 and 20), and snowpacks (*i.e.*, regions 21 and 23) become easily identifiable. Table 1 provides greater detail for each global region, including the number of sample sites, sampling location name, instrument methods employed, temporal range, and data citations. We have published metadata for each included article on the Zenodo data repository (see data availability) as an open access resource for researchers. This metadata will serve as a searchable index,<sup>20</sup> providing researchers with the ability to quickly query what records are available in specific global regions or time periods.





**Table 1** Pb records examined regionally. Regions are 20 first-order regions from the Global Terrestrial Network for Glaciers,<sup>64</sup> plus three author-defined regions. Note, references provided in ESI Table A.3 (ref. 20) and empty cells are denoted with a dash

Continent	Region (reg.) name	Reg. abv	Reg. code	Site count	Concentration	Isotope	Instrument method	Record type	Oldest sample	Youngest sample
Arctic	Greenland	GRL	05	60	x	x	IDMS; FAAS; CIM-ICP-MS; GC-MIP AED: GFAAS; FAAS; LEAFS; IC; ETAAS; ID-TIMS; INAA; LA-ICP-MS; TIMS; ICP-MS; DPASV	Ice; snow	250 000 BP	2014 CE
Arctic	Arctic Sea Ice	ASI	22	20	x	x	ICP-MS; TIMS; DPASV	Snow	1979 CE	2016 CE
Arctic	Arctic Canada	ACN	11	13	x	x	ICP-MS; LEAFS; ETV-ICP-MS; ETAAS	Ice; snow	15 815 BP	2004 CE
Arctic	North									
Arctic	Svalbard and Jan Mayen	SJM	07	5	—	x	TIMS	Snow	2016 CE	2016 CE
Arctic	Russian Arctic	RUA	09	1	x	—	CIM-ICP-MS	Ice	200 BCE	1999 CE
Arctic	Arctic Canada South	ACS	04	0	—	—	—	—	—	—
Arctic	Scandinavia	SCA	08	0	—	—	—	—	—	—
Asia	North Asia	ASN	10	45	x	x	ICP-MS; TIMS; GFAAS	Ice; snow	1680 CE	2021 CE
Asia	Central Asia	ASC	13	44	x	x	TIMS; ICP-MS	Ice; snow	~1150 CE	2016 CE
Asia	South Asia East	ASE	15	17	x	x	TIMS; ICP-MS	Ice; snow	~1450 CE	2010 CE
Asia	South Asia West	ASW	14	0	—	—	—	—	—	—
Asia	Caucasus and Middle East	CAU	12	0	—	—	—	—	—	—
Europe	Central Europe	CEU	03	11	x	x	CIM-ICP-MS; TIMS; ICP-MS; LA-ICP-MS; GFAAS	Ice; snow	3050 BCE	2019 CE
Europe	Baltic Sea	BAL	21	3	x	—	ICP-MS	Snow	2014 CE	2018 CE
Europe	Iceland	ISL	06	0	—	—	—	—	—	—
North America	Eastern Canada and USA	ENA	23	54	x	x	ICP-MS; TIMS	Snow	1997 CE	1998 CE
North America	Alaska	ALA	01	11	—	x	TIMS; ICP-MS	Ice; snow	1950 CE	2017 CE
North America	Western Canada and USA	WNA	02	7	x	x	CIM-ICP-MS; ICP-MS; TIMS	Ice; snow	8000 BP	2010 CE
Southern Hemisphere	Antarctic Mainland	ANT	20	243	x	x	ICP-MS; GFAAS; IDMS; ID-TIMS; LEAF-ETA; LEAFS; ETAAS; DPASV; TIMS; IDMS; ICP-OES	Ice; snow	672 000 BP	2020 CE
Southern Hemisphere	Subantarctic and Antarctic Islands	SAI	19	16	x	x	ICP-MS; GFAAS; ID-TIMS; ETAAS; DPASV; ICP-OES	Ice; snow	12 000 BP	2020 CE
Southern Hemisphere	Low latitudes	TRP	16	8	x	x	ICP-MS; CIM-ICP-MS	Ice	22 000 BP	1996 CE
Southern Hemisphere	Southern Andes	SAN	17	1	x	—	ICP-MS	Ice	1913 CE	2012 CE
Southern Hemisphere	New Zealand	NZL	18	0	—	—	—	—	—	—

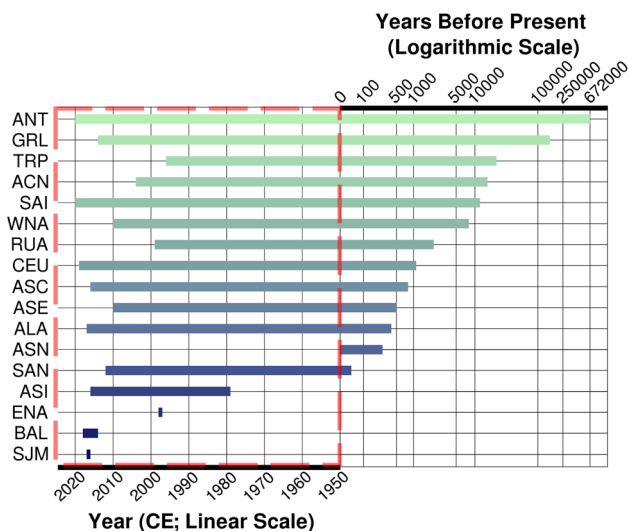


Fig. 4 Visualization of the temporal coverage of records for all glacier regions with records. Each glacier region is listed on the y-axis. There are two x-axes. To the left, in the red box, the x-axis corresponds to year (CE) on a linear scale. The time period from 2020 to 1950 CE has been plotted on a linear scale in the right panel, to provide greater visualization of small variations. On the right side, the second x-axis corresponded with time in years before the present (B.P.) on a logarithmic scale. The time period from 0 to 672 000 B.P. is presented in logarithmic scale to better visualize the long duration records from Antarctica and Greenland. See Table 1 for more details of regional temporal scales. From these plots, we see that the long ice core records from Antarctica and Greenland have the best temporal coverage. Eastern North America has the smallest temporal range of the regions with records, as the record consists entirely of snow collected from 1997 to 1998.

### 3.1 Spatial and temporal coverage of existing records

Examination of the spatial coverage of the global Pb records reveals the emergence of apparent data gaps. While mapped glaciers exist in Arctic Canada South, Iceland, Scandinavia, Caucasus and Middle East, South Asia West, and New Zealand, no Pb data has yet been reported from this ice or from snowpacks in these regions (Table 1). While data has been collected from all the other regions, the amount of data varies dramatically.

Pb concentration and isotopic analyses have been primarily focused (>15 records) on snow and ice in Antarctica, Greenland, Arctic Sea Ice, and the Tibetan Plateau, and on snowpacks in Eastern North America (Table 1). Some work (6–14 records) has been reported in Arctic Canada North, Central Europe, Alaska, Western North America, and the Low Latitudes (Table 1). Little data (1–5 records) exists for Svalbard and Jan Mayen, the Russian Arctic, the Baltic Sea, and the Southern Andes (Table 1).

Temporal coverage is also incredibly variable by region, which presents challenges to researchers (Fig. 3 and 4). Long ice cores recovered from Greenland and Antarctica span hundreds of thousands of years (Fig. 3 and 4; Table 1), providing insight into natural Pb fluctuation and examination of the first impacts of humans on the environment. Alpine glaciers stretch back only ~10 000 years (Table 1) but provide critical context to regional developments of culture, technology, and legislation

through regional Pb pollution sources. Regions with only snowpack data, tend to have the smallest temporal coverage (Fig. 3 and 4). The 54 records for Eastern North America represent only a year's Pb data – from 1997 to 1998 (Table 1). While many regions have Pb records spanning the start of the Industrial Revolution, few sites have been resampled to examine the change in Pb since the worldwide phase-out of leaded gasoline (Fig. 4). Even fewer have been sampled to record to the present (the 2020s), allowing researchers to see the effects of modern technology, legislation, and culture (e.g., the impact of the Covid-19 pandemic).

### 3.2 Analyzing gaps in available records

The collection of global long-range transported Pb records can only be utilized to its fullest potential in data-rich regions. Large data gaps make regional, inter-regional, and global comparisons difficult, if not impossible. Given the current spatial distribution of records (Fig. 3 and 4; Table 1), region-wide questions are only potentially accurate in regions that contain long temporal coverage and high spatial coverage. Typically, these two constrain potentially accurate regional data to regions with greater than five records. Recent work from Longman *et al.*<sup>66</sup> only used data from four regions in their regional analysis: Europe, Northeastern North America, the Central Andes, and Eastern Asia. One of the most pressing temporal data gaps is the absence of records existing post-1970. To make a rich comparison of the Arctic, Ardini *et al.* supplemented cryosphere records with other record types (sediment, peat, rock, biota, *etc.*) to have more complete spatial and temporal coverage.<sup>112</sup> Without complete records, researchers cannot accurately examine the impact of the phase-out of tetraethyl gasoline<sup>113</sup> and monitor new dominant Pb emission sources. Poor coverage spatially or temporally – “data gaps” – currently prohibit the accurate assessment of how Pb emissions change in most glacier regions (see Table 1) and worldwide over time.<sup>22,66</sup>

The data collection barriers must be understood to address the gaps in the published global Pb records. Early investigations of the snow and ice in low latitudes (glacial regions: SAN and TRP) primarily consisted of cores cut and melted in the field, with liquid samples prepared on-site for oxygen and hydrogen isotope, dust, and major cation and/or anion analysis. Critically, these procedures do not allow for decontamination, preventing accurate Pb and other metal analyses.<sup>80,95,114</sup> Therefore, the first reliable Pb data in tropical ice cores and snow were not gathered until 2001, when solid samples were recovered in Bolivia and transported to the laboratory for decontamination.<sup>115</sup> This shift in sampling procedure, while more costly, has mitigated critical data gaps in the low latitudes (ESI†<sup>20</sup>).<sup>81,93,115–119</sup>

Some ice cores collected and transported frozen for analysis have never been analyzed for Pb. Given the large number of analyses which are performed on ice cores (e.g., water isotopes, dust, trace elements, black carbon) on a finite amount of ice, it is key that proposed Pb analyses employ high sensitivity at low sample volumes. Researchers would fill spatial and temporal data gaps in published records by proposing to analyze ice already housed in archive facilities (e.g., the National Science



Foundation Ice Core Facility) without facing the cost of drilling a new ice core. Additionally, analysis of Pb on these cores would complement work already completed by researchers on the ice core site, broadening the drilling project's reach.

Ice core records from Greenland, Antarctica, and Europe provide a good understanding of past spikes in Pb emissions and emission signals verified through numerous sampling locations (Table 1). However, despite these direct assessments of the global Pb aerosol emissions, many of these ice core records have not been updated in 20 years. Of the sites examined (ESI†<sup>20</sup>), few Pb analysis records extend past 2010 or 2015. After the tetraethyl gasoline phase-out, industrial emission signals dominate,<sup>36,37</sup> clarifying the use and emission of Pb regionally.<sup>113</sup> Global Pb use, since the turn of the century, has shifted from North American and European industrialization to an emerging signal from China. Without direct data from ice cores and snowpacks, Pb emissions rely on governments' accurate self-reporting (Fig. 1 and citations therein). Extending records to the present would provide a greater understanding of ongoing global shifts in Pb emissions.

## 4 Using the records to answer research questions: a case study in the North Pacific

The power of this collection of global Pb records lies in its ability to quickly allow researchers to build regional, inter-regional, or global datasets. With these records, researchers can begin to ask regional or even global research questions about the effects of past regional development of technology and human culture on Pb composition and isotopes.<sup>66</sup> We illustrate this utility using the records to identify Pb records within the North Pacific region (Yukon Territory, Canada; Alaska, U.S.A.; Kamchatka Peninsula, Russia) and compare these with results from selected global sites.

The North Pacific contains over 86 000 km<sup>2</sup> of glaciers, making it one of the world's largest havens of non-polar ice.<sup>65</sup> 21st-century global climate change has dramatically affected this alpine region, with 3019 Gt of mass loss from Alaska alone from 1961 to 2016.<sup>120</sup> Alpine study sites in the North Pacific sample snow and aerosol (pollutant) deposition from both the Asian and North American continents,<sup>121</sup> allowing the study of Pacific climate processes and the examination of historical pollutant trends.<sup>6,51,114,122,123</sup> The aerosol plumes arriving in the North Pacific tend to contain large concentrations of anthropogenic aerosol particles. Contrary to the United States and Western Europe, which underwent industrialization from the mid-17th century to the early 19th century,<sup>23</sup> China has had several failed industrial revolutions before a successful mass production revolution from 1980 to the present.<sup>124</sup> Now an industrialized superpower globally, Chinese emissions have steadily increased (Fig. 1 and citations therein). Rising emissions are driven by population growth and industrialization without strict implementation of the breaking edge advances in engineering, which reduced atmospheric emissions from high-temperature smelting and refining processes.<sup>9,21</sup>

Examining the collated records, we see that several researchers working at sites across the North Pacific have reported Pb concentration and isotopes. At the Mt. Logan Prospector-Russell Col site (60.57 N, 140.41 W, 5300 m asl), a 186 m-long ice core was drilled to bedrock, yielding an 8000 year paleoclimate record of rising Pb concentrations.<sup>8</sup> In 2002, several shallow cores from Eclipse Icefield (60.51 N, 139.47 W, 3017 m asl) were recovered, and a 150 year Pb concentration and isotope ratio record was developed.<sup>51</sup> Snow pits collected across Alaska<sup>6,125,126</sup> and the St. Elias mountains<sup>127,128</sup> have been analyzed for Pb concentrations and isotope ratios at select depths. In this section, we will compare records from selected North Pacific publications<sup>6,8,51</sup> to key global records from (1) Summit, Greenland,<sup>7,53,55,73,80,129</sup> (2) East Rongbuk Glacier, Tibetan Plateau,<sup>61,63</sup> and (3) Dome Concordia, Antarctica.<sup>74,130–133</sup> To gather the data, we queried the collation of published long-range transported Pb records (Table 1, ESI†<sup>20</sup>) for eligible matches. We then examined the publication to ensure compatibility with our research question. Next, we gathered the Pb composition and isotope ratio data provided in each publication. Finally, we graphed the Pb concentration and isotope ratio data to identify regional, inter-regional, and global trends. Importantly, through this exercise, we will be able to establish what makes the North Pacific region unique.

Examining the Pb concentration values from the North Pacific and Greenland, the trends at each site illustrate unique regional trends. In Greenland, the rise in Pb concentration from 1760 till 1820 coincides with the First Industrial Revolution in Europe and North America.<sup>53,80,129</sup> As the Industrial Revolution grew and the demand for energy increased, Europe and North America turned to coal mining and consumption.<sup>134</sup> Coal was sourced from the United States, the British Isles, and Broken Hill, Australia.<sup>7</sup> The addition of tetraethyl Pb to gasoline in the 1920s is recorded as a large upswing in Pb concentration and in the <sup>206</sup>Pb/<sup>207</sup>Pb ratio, peaking in 1968 at  $236.31 \times 10^{-12} \text{ g g}^{-1}$ .<sup>129</sup> In 1967, the U.S. Clean Air Act restricted the addition of tetraethyl Pb in gasoline and limiting air pollution, sparking a global ban.<sup>135</sup> Pb concentrations recorded at Summit steadily decreased as a result.<sup>129</sup>

In the North Pacific, the trends observed in Greenland are not duplicated. From 5500 BCE (8000 BP) to 1500 CE, the average Pb concentration record is only  $5.57 \times 10^{-12} \text{ g g}^{-1}$ .<sup>8</sup> In 1500 CE, large spikes started to appear in Pb concentrations, up to  $30 \times 10^{-12} \text{ g g}^{-1}$ , associated with anthropogenic pollution.<sup>8</sup> However, the large rise in Pb concentration associated with the European and American industrial revolutions (1750s–1840s), continued rise due to coal mining and tetraethyl lead in gasoline, and fall associated with the banning of leaded gasoline is absent. Instead, the record remained relatively unchanged until the 1980s, when Pb concentration experienced a significant exponential increase from  $\sim 20$  to  $\sim 60 \times 10^{-12} \text{ g g}^{-1}$  in the 1970s<sup>8,51</sup> to  $226.57 \times 10^{-12} \text{ g g}^{-1}$  in 2001.<sup>51</sup> These records reflect China's industrial revolution in 1978 and the subsequent explosion of industrial output from China over the last 45 years.<sup>6,8,51,136</sup>

Examining Pb isotopes from the North Pacific as compared to other global regions (Fig. 5), we can see that the North Pacific







Fig. 5 Comparison of North Pacific<sup>8,53</sup> Pb isotope data to Dome Concordia, Antarctica,<sup>73,130–132</sup> East Rongbuk Glacier (Mt. Everest), Tibetan Plateau,<sup>50,63</sup> and Summit, Greenland.<sup>9,57,72</sup> No records are presented from South America due to a lack of available data. Panels (A–H) show slices of the data through time. Panel (A) shows data prior to 1770 (the preindustrial), (B) shows 1770–1920 (data from the European and American Industrial revolutions), and (C) shows 1920–1970 (Pb Gas Use). Panel (D–H) show decadal data progressively from the 1970s to the 2010s.

closely resembles the signal recorded in Greenland during the 1970s. Progressing from the 1970s through the 2010s, the Pb signal from the North Pacific drifts to higher, to more Asia-like,  $^{206}\text{Pb}/^{207}\text{Pb}$  values, providing a regionally unique signal for the North Pacific (Fig. 5 and references therein). Greenland records the impact of the United States and European leaded gasoline, coal, and aerosols on the environment from 1980 to 2008.<sup>7</sup>

However, as policy restricts Pb emission in North America and Europe at the end of the century, Greenland study sites begin to record the impact of Asian Pb pollution.<sup>7</sup> Conversely, the North Pacific strongly records the impact of Chinese and other Asian aerosols, ore, and coal Pb pollution signatures from the 1980s till 2001.<sup>6,51</sup> A lack of data before the 1970s prevents a rich inter-regional comparison during the pre-industrial, North American,



and European industrial revolutions, and Pb gas usage time frames. Filling this data gap is critical to determining if the pre-industrial signal from the North Pacific matches the closely clumped Asia, Greenland, and Antarctica records (Fig. 5, Panel A). While we would expect the North Pacific to resemble the Mt. Everest signal from 1770 till 1970, it is currently impossible to verify this hypothesis due to data availability (Fig. 5). Incomplete datasets temporally and spatially, not complete lack of data from South America, hinder a complete inter-regional or global comparison.

## 5 Conclusions and recommendations

Understanding Pb's global emission, transportation, and deposition is vital to mitigating its impact on human health and the environment. As Pb sources change, it is critical to continuously assess global Pb aerosol emissions. An understanding of published long-range transported Pb records analyzed from natural, undisturbed snowpacks and ice is required to track Pb deposition changes through time. The records collated for this systematic literature review (Table 1, ESI†<sup>20</sup>) will enable researchers to trace the connections between human action and Pb emission, leveraging recorded Pb isotope ratios as a method to fingerprint emission sources through time.

Immediate action is required to mitigate the endangerment of many high-altitude glaciers and the large temporal and spatial gaps in the current Pb data. Many of the sites endangered by climate change reside in regions where data is already scarce: low-latitude sites and mountain glaciers. To work within the constraints of climate change and funding agencies, we need to use a multi-faceted approach:

1. Some ice cores that have been collected and transported frozen for analysis and archive have never been analyzed for Pb. New analyses coupled with existing chronology would quickly begin to reduce regional and worldwide data gaps (*i.e.*, South America and Central Asia).
2. New proposals to work on snow and ice should be written to include Pb analyses. Researchers should work to reduce spatial gaps observed in the published records by sampling ice and snow from data-sparse regions in Table 1.
3. Previously studied sites must be revisited periodically to understand modern Pb emission sources and cultural effects. For example, an ice core retrieved in 1960 will not be able to record the transition from leaded to non-leaded gasoline.
4. Analyses should be non-destructive with low sample preparation requirements, high sensitivity, and capability for ultra-trace concentration Pb analysis, thereby preserving the sample for additional analysis types. Promising developments with cryo-LA-ICP-MS/MS, CIM-ICP-MS, ICP-TOF-MS, ICP-MS/MS, and SEM-EDS analyses make these requirements feasible.

A curated list of global long-traveled background atmospheric Pb records is crucial to researchers working to understand regional, inter-regional, and global anthropogenic impacts on the environment. Examining records from the cryosphere (ice and snow) allow researchers a unique opportunity to peer back in time and evaluate the direct impact of human society on Pb pollution emissions and sources. For this

to be successful, spatial and temporal data gaps need to be reduced. It is critical to complete this work presently, as climate change threatens the availability of cryosphere paleoclimate records. Effects of climate change in the cryosphere are heightened in regions with current spatial and temporal data gaps, adding pressure to collect Pb concentration and isotope ratio records quickly.

## Data availability

Data for this article are available on the Zenodo data repository at: <https://doi.org/10.5281/zenodo.7072483>. There are several files available: (1) individual sample site records, (2) traverse sample site records, (3) records grouped into 23 regions (full version of Table 1), (4) full citations of included records (as a text file and RIS), (5) additional figures and (6) systematic literature review methodology.<sup>22</sup>

## Author contributions

Hanna Brooks: visualization, data curation, writing – original draft preparation. Kimberley Miner: writing – reviewing and editing. Karl Kreutz: funding acquisition, conceptualization, writing – reviewing and editing. Dominic Winski: visualization, writing – reviewing and editing.

## Conflicts of interest

There are no conflicts to declare.

## Acknowledgements

The authors gratefully acknowledge the NOAA Air Resources Laboratory (A. R. L.) for providing the HYSPLIT transport and dispersion model used in this publication. This research was supported by National Science Foundation grants 2002483 and 2002470. The research was partially carried out at the Jet Propulsion Laboratory, California Institute of Technology, under a contract with the National Aeronautics and Space Administration (80NM0018D0004). Thanks to Nicholas Holschuh and Camden Bock for assistance plotting HYSPLIT trajectories in Python. Thanks to three anonymous reviewers, whose comments significantly enhanced this work.

## References

- 1 C. A. Sutherland, E. F. Milner, R. C. Kerby, H. Teindl and A. Melin, *Ullmann's encyclopedia of industrial chemistry, volume 19. Laboratory Information and Management Systems (LIMS) to Liquid-Liquid Extraction*, Wiley-VCH, Germany, 2003, vol. 19, pp. 323–370.
- 2 R. L. Rudnick and S. Gao, *Composition of the continental crust*, ed. H. D. Holland and K. K. Turekian, 2014.
- 3 H. Maring, D. M. Settle, P. Buat-Ménard, F. Dulac and C. C. Patterson, *Nature*, 1987, **330**, 154–156, DOI: [10.1038/330154a0](https://doi.org/10.1038/330154a0).



- 4 C. Barbante, A. Spolaor, W. R. Cairns and C. Boutron, *Earth-Sci. Rev.*, 2017, **168**, 218–231, DOI: [10.1016/j.earscirev.2017.02.010](https://doi.org/10.1016/j.earscirev.2017.02.010).
- 5 F. E. Grousset and P. E. Biscaye, *Chem. Geol.*, 2005, **222**, 149–167, DOI: [10.1016/j.chemgeo.2005.05.006](https://doi.org/10.1016/j.chemgeo.2005.05.006).
- 6 B. G. Koffman, P. Saylor, R. Zhong, L. Sethares, M. F. Yoder, L. Hanschka, T. Methven, Y. Cai, L. Bolge, J. Longman, S. L. Goldstein and E. C. Osterberg, *Environ. Sci. Technol.*, 2022, **56**, 13107–13118, DOI: [10.1021/acs.est.2c03767](https://doi.org/10.1021/acs.est.2c03767).
- 7 S. M. Wensman, A. E. Shiel and J. R. McConnell, *Anthropocene*, 2022, **38**, 100340, DOI: [10.1016/j.ancene.2022.100340](https://doi.org/10.1016/j.ancene.2022.100340).
- 8 E. Osterberg, P. Mayewski, K. Kreutz, D. Fisher, M. Handley, S. Sneed, C. Zdanowicz, J. Zheng, M. Demuth, M. Waskiewicz and J. Bourgeois, *Geophys. Res. Lett.*, 2008, **35**, L05810, DOI: [10.1029/2007GL032680](https://doi.org/10.1029/2007GL032680).
- 9 B. P. Bergman, *Geology and Medicine: Historical Connections*, ed. C. J. Duffin, C. Gardner-Thorpe and R. T. J. Moody, Geological Society, London, 2017, vol. 452, pp. 283–291, DOI: [10.1144/SP452.2](https://doi.org/10.1144/SP452.2).
- 10 P. Gabrielli and P. Vallelonga, *Environmental Contaminants: Using Natural Archives to Track Sources and Long-Term Trends of Pollution*, M. Blais, M. R. Rosen and J. P. Smol, 2015, vol. 18, pp. 393–430, DOI: [10.1007/978-94-017-9541-8\\_14](https://doi.org/10.1007/978-94-017-9541-8_14).
- 11 N. Silva-Sanchez and X. Armada, *Environ. Archaeol.*, 2023, **1**–25, DOI: [10.1080/14614103.2023.2181295](https://doi.org/10.1080/14614103.2023.2181295).
- 12 A. F. More, N. E. Spaulding, P. Bohleber, M. J. Handley, H. Hoffmann, E. V. Korotkikh, A. V. Kurbatov, C. P. Loveluck, S. B. Sneed, M. McCormick and P. A. Mayewski, *GeoHealth*, 2017, **1**, 211–219, DOI: [10.1002/2017GH000064](https://doi.org/10.1002/2017GH000064).
- 13 M. Krachler, J. Zheng, D. Fisher and W. Shotyk, *Anal. Chem.*, 2004, **76**, 5510–5517, DOI: [10.1021/ac0496190](https://doi.org/10.1021/ac0496190).
- 14 PNRA - Italian National Antarctic Programme, *Initial environment evaluation: The ice memory project*, 2024.
- 15 A. Mitra, I. Sen, S. Pandey, V. Velu, L. Reisberg, M. Bizimis, C. Cloquet and S. Nizam, *Environ. Sci. Technol.*, 2021, **55**, 13697–13708, DOI: [10.1021/acs.est.1c03830](https://doi.org/10.1021/acs.est.1c03830).
- 16 A. Zaborska, A. Strzelewicz, P. Rudnicka and M. Moskalik, *Mar. Pollut. Bull.*, 2020, **161**, 111719, DOI: [10.1016/j.marpolbul.2020.111719](https://doi.org/10.1016/j.marpolbul.2020.111719).
- 17 J. De Vera, P. Chandan, W. Landing, G. Stuppel, A. Steffen and B. Bergquist, *ACS Earth Space Chem.*, 2021, **5**, 2686–2699, DOI: [10.1021/acsearthspacechem.1c00132](https://doi.org/10.1021/acsearthspacechem.1c00132).
- 18 B. J. L. Jensen, L. J. Davies, C. Nolan, S. Pyne-O'Donnell, A. J. Monteath, V. Ponomareva, M. Portnyagin, R. Booth, M. Bursik, E. Cook, G. Plunkett, J. W. Vallance, Y. Luo, L. C. Cwynar, P. Hughes and D. G. Pearson, *Quat. Sci. Rev.*, 2021, **272**, 107242, DOI: [10.1016/j.quascirev.2021.107242](https://doi.org/10.1016/j.quascirev.2021.107242).
- 19 S. Krisch, O. Huhn, A. Al-Hashem, M. J. Hopwood, P. Lodeiro and E. P. Achterberg, *Geophys. Res. Lett.*, 2022, **49**, e2022GL100296, DOI: [10.1029/2022GL100296](https://doi.org/10.1029/2022GL100296).
- 20 H. L. Brooks, K. R. Miner, K. J. Kreutz and D. A. Winski, A Global Review of Long-range Transported Lead Concentration and Isotopic Ratio Records in Snow and Ice (Supplementary Data), Zenodo, [Data set], 2024, DOI: [10.5281/zenodo.7072483](https://doi.org/10.5281/zenodo.7072483).
- 21 J. M. Pacyna and E. G. Pacyna, *Environ. Rev.*, 2001, **9**, 269–298, DOI: [10.2307/envirevi.9.4.269](https://doi.org/10.2307/envirevi.9.4.269).
- 22 S. K. Marx, S. Rashid and N. Stromsoe, *Environ. Pollut.*, 2016, **213**, 283–298, DOI: [10.1016/j.envpol.2016.02.006](https://doi.org/10.1016/j.envpol.2016.02.006).
- 23 J. De Vries, *J. Econ. Hist.*, 1994, **54**, 249–270, DOI: [10.1017/S0022050700014467](https://doi.org/10.1017/S0022050700014467).
- 24 A. Guterres, *Secretary-general's message on the global phase-out of leaded petrol*, Intergovernmental Organization, 2021.
- 25 United States Environmental Protection Agency, 2008, *National emissions inventory (NEI) data*, 2013.
- 26 United States Environmental Protection Agency, 2011, *National emissions inventory (NEI) data*, 2014.
- 27 United States Environmental Protection Agency, 2014, *National emissions inventory (NEI) data*, 2016.
- 28 United States Environmental Protection Agency, 2017, *National emissions inventory (NEI) data*, 2020.
- 29 European Environment Agency, *National emissions reported to the convention on long-range transboundary air pollution (LRTAP convention)*, tech. rep. DAT-16-en, European Environment Agency, 2020.
- 30 Environment and Climate Change Canada, *Canada's air pollutant emissions inventory [Data set]*, 2020, fa1c88a8-bf78-4fcb-9c1e-2a5534b92131.
- 31 H. Z. Tian, C. Y. Zhu, J. J. Gao, K. Cheng, J. M. Hao, K. Wang, S. B. Hua, Y. Wang and J. R. Zhou, *Atmos. Chem. Phys.*, 2015, **15**, 10127–10147, DOI: [10.5194/acp-15-10127-2015](https://doi.org/10.5194/acp-15-10127-2015).
- 32 Q. Li, H. Cheng, T. Zhou, C. Lin and S. Guo, *Atmos. Environ.*, 2012, **60**, 1–8, DOI: [10.1016/j.atmosenv.2012.06.025](https://doi.org/10.1016/j.atmosenv.2012.06.025).
- 33 C. F. Boutron, U. Görlach, J.-P. Candelone, M. A. Bolshov and R. J. Delmas, *Nature*, 1991, **353**, 153–156, DOI: [10.1038/353153a0](https://doi.org/10.1038/353153a0).
- 34 L. J. Kristensen, *Atmos. Environ.*, 2015, **111**, 195–201, DOI: [10.1016/j.atmosenv.2015.04.012](https://doi.org/10.1016/j.atmosenv.2015.04.012).
- 35 L. D. Lacerda and M. G. Ribeiro, *J. Braz. Chem. Soc.*, 2004, **15**, 931–937, DOI: [10.1590/S0103-50532004000600022](https://doi.org/10.1590/S0103-50532004000600022).
- 36 A. Bollhöfer and K. J. R. Rosman, *Geochim. Cosmochim. Acta*, 2000, **64**, 3251–3262, DOI: [10.1016/S0016-7037\(00\)00436-1](https://doi.org/10.1016/S0016-7037(00)00436-1).
- 37 A. Bollhöfer and K. J. R. Rosman, *Geochim. Cosmochim. Acta*, 2001, **65**, 1727–1740, DOI: [10.1016/S0016-7037\(00\)00630-X](https://doi.org/10.1016/S0016-7037(00)00630-X).
- 38 J. De Laeter, *Mass Spectrom. Rev.*, 2011, **30**, 757–771, DOI: [10.1002/mas.20300](https://doi.org/10.1002/mas.20300).
- 39 K. A. Graeme and C. V. Pollack, *J. Emerg. Med.*, 1998, **16**, 171–177, DOI: [10.1016/s0736-4679\(97\)00283-7](https://doi.org/10.1016/s0736-4679(97)00283-7).
- 40 M. Balali-Mood, K. Naseri, Z. Tahergorabi, M. R. Khazdair and M. Sadeghi, *Front. Pharmacol.*, 2021, **12**, DOI: [10.3389/fphar.2021.643972](https://doi.org/10.3389/fphar.2021.643972).
- 41 L. Shahzad, M. Ali, H. Zubair, F. Sharif, M. Hayyat and G. Ghafoor, *Int. J. Environ. Anal. Chem.*, 2022, **1–13**, DOI: [10.1080/03067319.2022.2106433](https://doi.org/10.1080/03067319.2022.2106433).
- 42 D. Jaffe, I. McKendry, T. Anderson and H. Price, *Atmos. Environ.*, 2003, **37**, 391–404, DOI: [10.1016/S1352-2310\(02\)00862-2](https://doi.org/10.1016/S1352-2310(02)00862-2).
- 43 G. E. Shaw, *Rev. Geophys.*, 1988, **26**, 89–112, DOI: [10.1029/RG026i001p00089](https://doi.org/10.1029/RG026i001p00089).



- 44 C. Papastefanou, *Appl. Radiat. Isot.*, 2006, **64**, 93–100, DOI: [10.1016/j.apradiso.2005.07.006](https://doi.org/10.1016/j.apradiso.2005.07.006).
- 45 W. T. Sturges and L. A. Barrie, *Nature*, 1987, **329**, 144–146, DOI: [10.1038/329144a0](https://doi.org/10.1038/329144a0).
- 46 J. Anzano, E. Abás, C. Marina-Montes, J. del Valle, D. Galán-Madruga, M. Laguna, S. Cabredo, L.-V. Pérez-Arribas, J. Cáceres and J. Anwar, *Atmosphere*, 2022, **13**(10), 1621, DOI: [10.3390/atmos13101621](https://doi.org/10.3390/atmos13101621).
- 47 M. Nishikawa, S. Kanamori, N. Kanamori and T. Mizoguchi, *Sci. Total Environ.*, 1991, **107**, 13–27, DOI: [10.1016/0048-9697\(91\)90247-C](https://doi.org/10.1016/0048-9697(91)90247-C).
- 48 A. Svensson, S. Fujita, M. Bigler, M. Braun, R. Dallmayr, V. Gkinis, K. Goto-Azuma, M. Hirabayashi, K. Kawamura, S. Kipfstuhl, H. A. Kjaer, T. Popp, M. Simonsen, J. P. Steffensen, P. Vallelonga and B. M. Vinther, *Climate of the Past*, 2015, **11**, 1127–1137, DOI: [10.5194/cp-11-1127-2015](https://doi.org/10.5194/cp-11-1127-2015).
- 49 A. F. Stein, R. R. Draxler, G. D. Rolph, B. J. B. Stunder, M. D. Cohen and F. Ngan, *Bull. Am. Meteorol. Soc.*, 2015, **96**, 2059–2077, DOI: [10.1175/BAMS-D-14-00110.1](https://doi.org/10.1175/BAMS-D-14-00110.1).
- 50 G. Rolph, A. Stein and B. Stunder, *Environ. Model. Software*, 2017, **95**, 210–228, DOI: [10.1016/j.envsoft.2017.06.025](https://doi.org/10.1016/j.envsoft.2017.06.025).
- 51 B. H. Gross, K. J. Kreutz, E. C. Osterberg, J. R. McConnell, M. Handley, C. P. Wake and K. Yalcin, *J. Geophys. Res.: Atmos.*, 2012, **117**, DOI: [10.1029/2011JD017270](https://doi.org/10.1029/2011JD017270).
- 52 J. R. McConnell, A. I. Wilson, A. Stohl, M. M. Arienzo, N. J. Chellman, S. Eckhardt, E. M. Thompson, A. M. Pollard and J. P. Steffensen, *Proc. Natl. Acad. Sci. U. S. A.*, 2018, **115**, 5726–5731, DOI: [10.1073/pnas.1721818115](https://doi.org/10.1073/pnas.1721818115).
- 53 J. R. McConnell and R. Edwards, *Proc. Natl. Acad. Sci. U. S. A.*, 2008, **105**, 12140–12144, DOI: [10.1073/pnas.0803564105](https://doi.org/10.1073/pnas.0803564105).
- 54 K. J. R. Rosman, W. Chisholm, C. F. Boutron, J. P. Candelone and S. Hong, *Geochim. Cosmochim. Acta*, 1994, **58**, 3265–3269, DOI: [10.1016/0016-7037\(94\)90054-X](https://doi.org/10.1016/0016-7037(94)90054-X).
- 55 K. J. R. Rosman, W. Chisholm, S. Hong, J. P. Candelone and C. F. Boutron, *Environ. Sci. Technol.*, 1997, **31**, 3413–3416, DOI: [10.1021/es970038k](https://doi.org/10.1021/es970038k).
- 56 P. De Deckker, *Earth-Sci. Rev.*, 2019, **194**, 536–567, DOI: [10.1016/j.earscirev.2019.01.008](https://doi.org/10.1016/j.earscirev.2019.01.008).
- 57 J. R. McConnell, O. J. Maselli, M. Sigl, P. Vallelonga, T. Neumann, H. Anshütz, R. C. Bales, M. A. Curran, S. B. Das, R. Edwards, S. Kipfstuhl, L. Layman and E. R. Thomas, *Sci. Rep.*, 2014, **4**, 5848, DOI: [10.1038/srep05848](https://doi.org/10.1038/srep05848).
- 58 F. A. M. Planchon, K. van de Velde, K. J. R. Rosman, E. W. Wolff, C. P. Ferrari and C. F. Boutron, *Geochim. Cosmochim. Acta*, 2003, **67**, 693–708, DOI: [10.1016/S0016-7037\(02\)01136-5](https://doi.org/10.1016/S0016-7037(02)01136-5).
- 59 K. Rosman, *Australian Antarctic Data Centre*, 2000, DOI: [10.4225/15/548a578d63b5e](https://doi.org/10.4225/15/548a578d63b5e).
- 60 P. Vallelonga, P. Gabrielli, E. Balliana, A. Wegner, B. Delmonte, C. Turetta, G. Burton, F. Vanhaecke, K. J. R. Rosman, S. Hong, C. F. Boutron, P. Cescon and C. Barbante, *NOAA Paleoclimatology*, 2011.
- 61 L. Burn-Nunes, P. Vallelonga, K. Lee, S. Hong, G. Burton, S. Hou, A. Moy, R. Edwards, R. Loss and K. Rosman, *Sci. Total Environ.*, 2014, **487**, 407–419, DOI: [10.1016/j.scitotenv.2014.03.120](https://doi.org/10.1016/j.scitotenv.2014.03.120).
- 62 A. Eichler, L. Tobler, S. Eyrikh, G. Gramlich, N. Malygina, T. Papina and M. Schwikowski, *Environ. Sci. Technol.*, 2012, **46**, 4323–4330, DOI: [10.1021/es2039954](https://doi.org/10.1021/es2039954).
- 63 K. Lee, S. D. Hur, S. Hou, L. J. Burn-Nunes, S. Hong, C. Barbante, C. F. Boutron and K. J. Rosman, *Environ. Sci. Technol.*, 2011, **412–413**, 194–202, DOI: [10.1016/j.scitotenv.2011.10.002](https://doi.org/10.1016/j.scitotenv.2011.10.002).
- 64 Global Terrestrial Network for Glaciers (GTN-G), *GTN-g glacier regions (GlacReg)*, 2023, DOI: [10.5904/gtng-glacreg-2023-07](https://doi.org/10.5904/gtng-glacreg-2023-07).
- 65 RGI 7.0 Consortium, *Randolph glacier inventory - a dataset of global glacier outlines, version 7.0.*, Boulder, Colorado, USA, 2023, DOI: [doi:10.5067/f6jmovy5navz](https://doi.org/10.5067/f6jmovy5navz).
- 66 J. Longman, V. Ersek and D. Veres, *Sci. Rep.*, 2020, **10**, 20890, DOI: [10.1038/s41598-020-77773-w](https://doi.org/10.1038/s41598-020-77773-w).
- 67 M. Błaś, K. Cichała-Kamrowska, M. Sobik, X. Polkowska and J. Namieśnik, *Environ. Rev.*, 2010, **18**, 87–114, DOI: [10.1139/A10-003](https://doi.org/10.1139/A10-003).
- 68 E. W. Wolff, *Antarct. Sci.*, 2005, **17**, 487–495, DOI: [10.1017/S0954102005002919](https://doi.org/10.1017/S0954102005002919).
- 69 D. Weiss, W. Shotyk and O. Kempf, *Naturwissenschaften*, 1999, **86**, 262–275, DOI: [10.1007/s001140050612](https://doi.org/10.1007/s001140050612).
- 70 K. R. Miner, S. Campbell, C. Gerbi, A. Liljedahl, T. Anderson, L. B. Perkins, S. Bernsen, T. Gatesman and K. J. Kreutz, *Water*, 2018, **10**, 1157, DOI: [10.3390/w10091157](https://doi.org/10.3390/w10091157).
- 71 J. R. Hawkings, M. L. Skidmore, J. L. Wadham, J. C. Prisco, P. L. Morton, J. E. Hatton, C. B. Gardner, T. J. Kohler, M. Stibal, E. A. Bagshaw, A. Steigmeyer, J. Barker, J. E. Dore, W. B. Lyons, M. Tranter, R. G. M. Spencer and the SALSA Science Team, *Proc. Natl. Acad. Sci. U. S. A.*, 2020, **117**, 31648–31659, DOI: [10.1073/pnas.2014378117](https://doi.org/10.1073/pnas.2014378117).
- 72 I. Kim, G. Kim and E. J. Choy, *Polar Res.*, 2015, **34**, 24289, DOI: [10.3402/polar.v34.24289](https://doi.org/10.3402/polar.v34.24289).
- 73 G. R. Burton, K. J. R. Rosman, J.-P. Candelone, L. J. Burn, C. F. Boutron and S. Hong, *Earth Planet. Sci. Lett.*, 2007, **259**, 557–566, DOI: [10.1016/j.epsl.2007.05.015](https://doi.org/10.1016/j.epsl.2007.05.015).
- 74 C. Han, L. J. Burn, P. Vallelonga, S. D. Hur, C. F. Boutron, Y. Han, S. Lee, A. Lee and S. Hong, *Molecules*, 2022, **27**, 4208, DOI: [10.3390/molecules27134208](https://doi.org/10.3390/molecules27134208).
- 75 A. Simonetti, C. Garipey and J. Carignan, *Geochim. Cosmochim. Acta*, 2000, **64**, 5–20, DOI: [10.1016/S0016-7037\(99\)00207-0](https://doi.org/10.1016/S0016-7037(99)00207-0).
- 76 A. Simonetti, C. Garipey and J. Carignan, *Geochim. Cosmochim. Acta*, 2000, **64**, 3439–3452, DOI: [10.1016/S0016-7037\(00\)00446-4](https://doi.org/10.1016/S0016-7037(00)00446-4).
- 77 D. P. West and D. R. Lux, *Earth Planet. Sci. Lett.*, 1993, **120**, 221–237, DOI: [10.1016/0012-821X\(93\)90241-Z](https://doi.org/10.1016/0012-821X(93)90241-Z).
- 78 D. Wen-tao, K. Shi-chang, Q. Xiang, S. Wei-jun, Z. Yu-lan, L. Yu-shuo and C. Ji-zu, *J. Mt. Sci.*, 2018, **15**, 1950–1960, DOI: [10.1007/s11629-017-4679-2](https://doi.org/10.1007/s11629-017-4679-2).
- 79 P. Ginot, J. Chappellaz, C. Barbante, M. Schwikowski and A.-C. Ohlmann, *Ice Memory, EGU General Assembly Conference Abstracts*, 2021, EGU21-8842, DOI: [10.5194/egusphere-egu21-8842](https://doi.org/10.5194/egusphere-egu21-8842).





- 80 J.-P. Candelone, S. Hong and C. F. Boutron, *Anal. Chim. Acta*, 1994, **299**, 9–16, DOI: [10.1016/0003-2670\(94\)00327-0](https://doi.org/10.1016/0003-2670(94)00327-0).
- 81 S. Hong, C. Barbante, C. Boutron, P. Gabrielli, V. Gaspari, P. Cescon, L. Thompson, C. Ferrari, B. Francou and L. Maurice-Bourgoin, *J. Environ. Monit.*, 2004, DOI: [10.1039/b314251e](https://doi.org/10.1039/b314251e).
- 82 M. Murozumi, T. J. Chow and C. Patterson, *Geochim. Cosmochim. Acta*, 1969, **33**, 1247–1294, DOI: [10.1016/0016-7037\(69\)90045-3](https://doi.org/10.1016/0016-7037(69)90045-3).
- 83 A. Ng and C. Patterson, *Geochim. Cosmochim. Acta*, 1981, **45**, 2109–2121, DOI: [10.1016/0016-7037\(81\)90064-8](https://doi.org/10.1016/0016-7037(81)90064-8).
- 84 C. Patterson, J. Ericson, M. Manea-Krichthen and H. Shirahata, *Sci. Total Environ.*, 1991, **107**, 205–236, DOI: [10.1016/0048-9697\(91\)90260-1](https://doi.org/10.1016/0048-9697(91)90260-1).
- 85 B. Guo, J. Wang, C. Lin, M. He and W. Ouyang, *Chemosphere*, 2019, **227**, 225–236, DOI: [10.1016/j.chemosphere.2019.04.047](https://doi.org/10.1016/j.chemosphere.2019.04.047).
- 86 C. Rosca, R. Schoenberg, E. L. Tomlinson and B. S. Kamber, *Sci. Total Environ.*, 2019, **658**, 234–249, DOI: [10.1016/j.scitotenv.2018.12.049](https://doi.org/10.1016/j.scitotenv.2018.12.049).
- 87 F. Arnaud, M. Revel-Rolland, D. Bosch, T. Winiareki, M. Desmet, N. Tribouvillard and N. Givélet, *J. Environ. Monit.*, 2004, DOI: [10.1039/b314947a](https://doi.org/10.1039/b314947a).
- 88 R. Bindler, I. Renberg, N. J. Anderson, P. G. Appleby, O. Emteryd and J. Boyle, *Atmos. Environ.*, 2001, **35**, 4675–4685, DOI: [10.1016/S1352-2310\(01\)00115-7](https://doi.org/10.1016/S1352-2310(01)00115-7).
- 89 F. Ardini, A. Bazzano and M. Grotti, *J. Anal. At. Spectrom.*, 2018, **33**, 2124–2132, DOI: [10.1039/c8ja00296g](https://doi.org/10.1039/c8ja00296g).
- 90 A. Bazzano and M. Grotti, *J. Anal. At. Spectrom.*, 2014, **29**, 926–933, DOI: [10.1039/c3ja50388g](https://doi.org/10.1039/c3ja50388g).
- 91 D. Della Lunga, W. Müller, S. O. Rasmussen and A. Svensson, *J. Glaciol.*, 2014, **60**, 970–988, DOI: [10.3189/2014JG13J199](https://doi.org/10.3189/2014JG13J199).
- 92 D. Della Lunga, W. Müller, S. O. Rasmussen, A. Svensson and P. Vallelonga, *Cryosphere*, 2017, **11**, 1297–1309, DOI: [10.5194/tc-11-1297-2017](https://doi.org/10.5194/tc-11-1297-2017).
- 93 S. Knüsel, D. E. Piguet, M. Schwikowski and H. W. Gäggeler, *Environ. Sci. Technol.*, 2003, **37**, 2267–2273, DOI: [10.1021/es026452o](https://doi.org/10.1021/es026452o).
- 94 A. Martín-Esteban and B. Slowikowski, *Crit. Rev. Anal. Chem.*, 2003, **33**, 43–55, DOI: [10.1080/713609153](https://doi.org/10.1080/713609153).
- 95 J. R. McConnell, G. W. Lamorey, S. W. Lambert and K. C. Taylor, *Environ. Sci. Technol.*, 2002, **36**, 7–11, DOI: [10.1021/es011088z](https://doi.org/10.1021/es011088z).
- 96 W. Müller, J. M. G. Shelley and S. O. Rasmussen, *J. Anal. At. Spectrom.*, 2011, **26**(12), 2391–2395, DOI: [10.1039/c1ja10242g](https://doi.org/10.1039/c1ja10242g).
- 97 H. Reinhardt, M. Kriews, H. Miller, O. Schrems, C. Lüdke, E. Hoffmann and J. Skole, *Anal. Bioanal. Chem.*, 2001, **370**, 629–636, DOI: [10.1007/s002160100853](https://doi.org/10.1007/s002160100853).
- 98 S. B. Sneed, P. A. Mayewski, W. G. Sayre, M. J. Handley, A. V. Kurbatov, K. C. Taylor, P. Bohleber, D. Wagenbach, T. Erhardt and N. E. Spaulding, *J. Glaciol.*, 2015, **61**, 233–242, DOI: [10.3189/2015JG14J139](https://doi.org/10.3189/2015JG14J139).
- 99 R. E. Sturgeon, S. N. Willie, J. Zheng, A. Kudo and D. C. Gregoire, *J. Anal. At. Spectrom.*, 1993, **8**, 6, DOI: [10.1039/JA9930801053](https://doi.org/10.1039/JA9930801053).
- 100 A. Makishima and E. Nakamura, *J. Anal. At. Spectrom.*, 2010, **25**, 1712, DOI: [10.1039/c0ja00015a](https://doi.org/10.1039/c0ja00015a).
- 101 M. Krachler, J. Zheng, R. Koerner, C. Zdanowicz, D. Fisher and W. Shotyk, *J. Environ. Monit.*, 2005, **7**, 1169–1176, DOI: [10.1039/b509373b](https://doi.org/10.1039/b509373b).
- 102 F. Pawlak, K. Koziol and Z. Polkowska, *Sci. Total Environ.*, 2021, **778**, 145244, DOI: [10.1016/j.scitotenv.2021.145244](https://doi.org/10.1016/j.scitotenv.2021.145244).
- 103 D. Dick, A. Wegner, P. Gabrielli, U. Ruth, C. Barbante and M. Kriews, *Anal. Chim. Acta*, 2008, **621**, 140–147, DOI: [10.1016/j.aca.2008.05.026](https://doi.org/10.1016/j.aca.2008.05.026).
- 104 W. Chisholm, K. J. R. Rosman, C. F. Boutron, J. P. Candelone and S. Hong, *Anal. Chim. Acta*, 1995, **311**, 141–151, DOI: [10.1016/0003-2670\(95\)00181-X](https://doi.org/10.1016/0003-2670(95)00181-X).
- 105 I. Bajenaru, A. Josceanu, C. Guran and I. Minca, *Rev. Chim.*, 2015, **66**, 1960–1964.
- 106 C. F. Boutron, M. A. Bolshov, S. N. Rudniev, F. P. Hartmann, B. Hutch and N. I. Barkov, *J. Phys. IV*, 1991, **1**, C7, DOI: [10.1051/jp4:19917186](https://doi.org/10.1051/jp4:19917186).
- 107 S. I. Jimi, K. J. R. Rosman, S. Hong, J.-P. Candelone, L. J. Burn and C. F. Boutron, *Anal. Bioanal. Chem.*, 2008, **390**, 495–501, DOI: [10.1007/s00216-007-1729-6](https://doi.org/10.1007/s00216-007-1729-6).
- 108 P. Vallelonga, K. Van de Velde, J. P. Candelone, C. Ly, K. J. R. Rosman, C. F. Boutron, V. I. Morgan and D. J. Mackey, *Anal. Chim. Acta*, 2002, **453**, 1–12, DOI: [10.1016/S0003-2670\(01\)01490-8](https://doi.org/10.1016/S0003-2670(01)01490-8).
- 109 L. J. Burn, K. J. R. Rosman, J.-P. Candelone, P. Vallelonga, G. R. Burton, A. M. Smith, V. I. Morgan, C. Barbante, S. Hong and C. F. Boutron, *Anal. Chim. Acta*, 2009, **634**, 228–236, DOI: [10.1016/j.aca.2008.11.067](https://doi.org/10.1016/j.aca.2008.11.067).
- 110 F. Esaka, K. Watanabe, M. Magara and S. Usuda, *Instrum. Sci. Technol.*, 2004, **32**, 103–114, DOI: [10.1081/CI-120028764](https://doi.org/10.1081/CI-120028764).
- 111 N. Nagatsuka, K. Goto-Azuma, A. Tsushima, K. Fujita, S. Matoba, Y. Onuma, M. Kadota, M. Minowa, Y. Komuro, H. Motoyama and T. Aoki, *Clim. Past Discuss*, 2021, **17**, 1341–1361, DOI: [10.5194/cp-2020-146](https://doi.org/10.5194/cp-2020-146).
- 112 F. Ardini, A. Bazzano and M. Grotti, *Environ. Chem.*, 2020, **17**, 213–239, DOI: [10.1071/EN19227](https://doi.org/10.1071/EN19227).
- 113 U. N. E. Programme, *The lead campaign*, 2017.
- 114 E. C. Osterberg, M. J. Handley, S. B. Sneed, P. A. Mayewski and K. J. Kreutz, *Environ. Sci. Technol.*, 2006, **40**, 3355–3361, DOI: [10.1021/es052536w](https://doi.org/10.1021/es052536w).
- 115 C. P. Ferrari, T. Clotteau, L. G. Thompson, C. Barbante, G. Cozzi, P. Cescon, S. Hong, L. Maurice-Bourgoin, B. Francou and C. F. Boutron, *Atmos. Environ.*, 2001, **35**, 5809–5815, DOI: [10.1016/S1352-2310\(01\)00347-8](https://doi.org/10.1016/S1352-2310(01)00347-8).
- 116 A. Eichler, G. Gramlich, T. Kellerhals, L. Tobler and M. Schwikowski, *Sci. Adv.*, 2015, **1**, DOI: [10.1126/sciadv.1400196](https://doi.org/10.1126/sciadv.1400196).
- 117 M. Potocki, D. A. Dixon, A. V. Kurbatov, G. Casassa, R. Zamora, M. J. Handley, D. Introne, B. Grigholm, E. V. Korotkikh, S. D. Birkel, H. Clifford and P. A. Mayewski, *Atmos. Environ.*, 2022, **276**, 119002, DOI: [10.1016/j.atmosenv.2022.119002](https://doi.org/10.1016/j.atmosenv.2022.119002).
- 118 C. Uglietti, P. Gabrielli, J. W. Olesik, A. Lutton and L. G. Thompson, *Appl. Geochem.*, 2014, **47**, 109–121, DOI: [10.1016/j.apgeochem.2014.05.019](https://doi.org/10.1016/j.apgeochem.2014.05.019).



- 119 C. Uglietti, P. Gabrielli, C. A. Cooke, P. Vallenga and L. G. Thompson, *Proc. Natl. Acad. Sci. U. S. A.*, 2015, **112**, 2349–2354.
- 120 M. Zemp, M. Huss, E. Thibert, N. Eckert, R. McNabb, J. Huber, M. Barandun, H. Machguth, S. U. Nussbaumer, I. Gärtner-Roer, L. Thomson, F. Paul, F. Maussion, S. Kutuzov and J. G. Cogley, *Nature*, 2019, **568**, 382–398, DOI: [10.1038/s41586-019-1071-0](https://doi.org/10.1038/s41586-019-1071-0).
- 121 T. J. Yasunari, T. Shiraiwa, S. Kanamori, Y. Fujii, M. Igarashi, K. Yamazaki, C. S. Benson and T. Hondoh, *J. Geophys. Res.: Atmos.*, 2007, **112**(D10), DOI: [10.1029/2006JD008121](https://doi.org/10.1029/2006JD008121).
- 122 D. Winski, E. Osterberg, D. Ferris, K. Kreutz, C. Wake, S. Campbell, R. Hawley, S. Roy, S. Birkel, D. Introne and M. Handley, *Sci. Rep.*, 2017, **7**, 17869, DOI: [10.1038/s41598-017-18022-5](https://doi.org/10.1038/s41598-017-18022-5).
- 123 C. Zdanowicz, D. Fisher, J. Bourgeois, M. Demuth, J. Zheng, P. Mayewski, K. Kreutz, E. Osterberg, K. Yalcin, C. Wake, E. J. Steig, D. Froese and K. Goto-Azuma, *Arctic*, 2014, **67**, 35–57, DOI: [10.14430/arctic4352](https://doi.org/10.14430/arctic4352).
- 124 M. Dutta, *China's industrial revolution and economic presence*, World Scientific Publishing Company, Singapore, Singapore, 2005.
- 125 Z. Du, C. Xiao, T. Dou, S. Li, H. An, S. Liu and K. Liu, *Atmos. Environ.*, 2019, **214**, 116837, DOI: [10.1016/j.atmosenv.2019.116837](https://doi.org/10.1016/j.atmosenv.2019.116837).
- 126 T. K. Hinkley, *J. Geophys. Res.: Atmos.*, 1993, **98**, 20537–20545, DOI: [10.1029/93JD02257](https://doi.org/10.1029/93JD02257).
- 127 A. J.-M. Bory, W. Abouchami, S. J. G. Galer, A. Svensson, J. N. Christensen and P. E. Biscaye, *Environ. Sci. Technol.*, 2014, **48**, 1451–1457, DOI: [10.1021/es4035655](https://doi.org/10.1021/es4035655).
- 128 C. Zdanowicz, G. Hall, J. Vaive, Y. Amelin, J. Percival, I. Girard, P. Biscaye and A. Bory, *Geochim. Cosmochim. Acta*, 2006, **70**, 3493–3507, DOI: [10.1016/j.gca.2006.05.005](https://doi.org/10.1016/j.gca.2006.05.005).
- 129 J. R. McConnell, N. J. Chellman, A. I. Wilson, A. Stohl, M. M. Arienzo, S. Eckhardt, D. Fritzsche, S. Kipfstuhl, T. Opel, P. F. Place and J. P. Steffensen, *Proc. Natl. Acad. Sci. U. S. A.*, 2019, **116**, 14910–14915, DOI: [10.1073/pnas.1904515116](https://doi.org/10.1073/pnas.1904515116).
- 130 A. Bazzano, K. Latruwe, M. Grotti and F. Vanhaecke, *J. Anal. At. Spectrom.*, 2015, **30**, 1322–1328, DOI: [10.1039/c4ja00484a](https://doi.org/10.1039/c4ja00484a).
- 131 S. Bertinetti, F. Ardini, M. A. Vecchio, L. Caiazza and M. Grotti, *Chemosphere*, 2020, **255**, 126858, DOI: [10.1016/j.chemosphere.2020.126858](https://doi.org/10.1016/j.chemosphere.2020.126858).
- 132 P. Vallenga, P. Gabrielli, K. J. R. Rosman, C. Barbante and C. F. Boutron, *Geophys. Res. Lett.*, 2005, **32**, L01706, DOI: [10.1029/2004GL021449](https://doi.org/10.1029/2004GL021449).
- 133 P. Vallenga, P. Gabrielli, E. Balliana, A. Wegner, B. Delmonte, C. Turetta, G. Burton, F. Vanhaecke, K. J. Rosman, S. Hong, C. F. Boutron, P. Cescon and C. Barbante, *Quat. Sci. Rev.*, 2010, **29**, 247–255, DOI: [10.1016/j.quascirev.2009.06.019](https://doi.org/10.1016/j.quascirev.2009.06.019).
- 134 R. Burt, *Econ. Hist. Rev.*, 1969, **22**, 249–268, DOI: [10.2307/2593770](https://doi.org/10.2307/2593770).
- 135 117th Congress, Clean Air Act 42 U.S.C. sect. 7401-7671q, 2022.
- 136 Y. Wen and G. E. Fortier, *J. Chin. Econ. Bus. Stud.*, 2019, **17**, 9–45, DOI: [10.1080/14765284.2019.1582224](https://doi.org/10.1080/14765284.2019.1582224).

